Optics Letters

Multi-access fiber-optic radio frequency transfer with passive phase noise compensation

Hongwei Li,[1] Guiling Wu,[1,2,*] Jiapeng Zhang,[1] Jianguo Shen,[3] and Jianping Chen[1,2]

[1]State Key Laboratory of Advanced Optical Communication Systems and Networks, Department of Electronic Engineering, Shanghai Jiao Tong University, Shanghai 200240, China
[2]Shanghai Key Laboratory of Navigation and Location-Based Services, Shanghai 200240, China
[3]College of Mathematics, Physics and Information Engineering, Zhejiang Normal University, Jinhua, Zhejiang 321004, China
*Corresponding author: wuguiling@sjtu.edu.cn

Received 12 October 2016; revised 5 November 2016; accepted 13 November 2016; posted 14 November 2016 (Doc. ID 278384); published 5 December 2016

In this Letter, we propose and demonstrate a multi-access fiber-optic radio frequency dissemination with passive phase noise cancelation. A forward phase-conjugated signal is generated at the local site by frequency mixing between the standard signal and the round-trip probe signal. A stable frequency signal is achieved by frequency mixing the tapped forward phase-conjugated signal and the backward probe signal at an arbitrary point along the fiber link. Different wavelengths for forward and backward directions are employed to efficiently suppress the effect of backscattering. At the same time, the increase of bidirectional asymmetry with the increase of user ends is avoided by employing the same wavelengths for all user ends. A multi-access frequency transfer over a 45 km fiber link based on the proposed scheme is demonstrated. The radio frequency signals with relative frequency stabilities of $10^{-17}/20{,}000$ s level are reproduced at two points of 5 and 40 km far from the local site along the fiber link, respectively. © 2016 Optical Society of America

OCIS codes: (060.2360) Fiber optics links and subsystems; (060.5625) Radio frequency photonics; (120.3940) Metrology.

https://doi.org/10.1364/OL.41.005672

Fiber-optic frequency transfer has been considered as a promising way to realize stable and long-distance radio frequency (RF) dissemination for many applications, such as navigation, long baseline interferometers, and radio astronomy [1]. Compared to satellite links, fiber links have higher stability (especially in the short term), anti-electromagnetic Interference, and lower attenuation. The temperature variation and mechanical perturbation along the fiber links, however, will still change the propagation delay of the fiber links and, hence, add extra phase noises into the transferred frequency signal [2]. Active compensation schemes [3–5] and passive compensation schemes [6–10] have been proposed to cancel the additional phase noises caused by the fluctuation of fiber link. Active compensation requires high precise phase error measurement, and fast and large-range compensators. Passive compensation schemes can achieve an endless dynamic range and fast-phase noise cancellation by simple phase-conjugate frequency mixing.

In order to support the applications with multiple users, two kinds of point-to-multipoint fiber-optic RF dissemination schemes have been proposed and demonstrated [11–16]. One is over branching fiber optical networks with phase noise compensation at each user end. In order to distinguish the round-trip signals of each user, different wavelengths [14,15] or RF frequencies [13] need to be employed for different user ends. An alternative method to distinguish the round-trip signals for different user ends is to directly reflect each round-trip signal at the corresponding branch [16]. In these schemes, the round-trip signal for each user is often carried on the same wavelength to avoid multiple optical-electrical and electrical-optical conversion at the local site. However, it will introduce undistinguished backscattering noises. The other kind of distributed RF dissemination scheme is over multi-access fiber optical networks with active phase noise compensation at the local site [11,12]. The stable frequency signal is obtained from the taped forward and backward signals at an arbitrary point along the fiber link. In this letter, we propose a multi-access fiber-optic RF transfer scheme with passive phase noise compensation. At the local site, a forward phase-conjugated signal is generated by frequency mixing the standard signal and the round-trip probe signal. At an arbitrary point along the fiber link, the forward phase-conjugated signal and backward probe signal are tapped and mixed to derive a stable frequency signal. The effect of backscattering can be efficiently suppressed by employing different wavelengths for the forward and backward directions. A multi-access frequency transfer over a 45 km fiber link based on the proposed scheme is demonstrated. The RF transfer stabilities of $10^{-17}/20{,}000$ s levels are obtained at two user ends along the main link.

Figure 1 illustrates the diagram of the proposed scheme. At the local site, the standard RF signal is split into two branches by a power splitter (PS). One branch is divided by two as the probe signal and then modulated on an optical carrier (λ_1) to be transmitted to the remote site. At the remote site, the signal carried on λ_1 is photodetected and transmitted back along

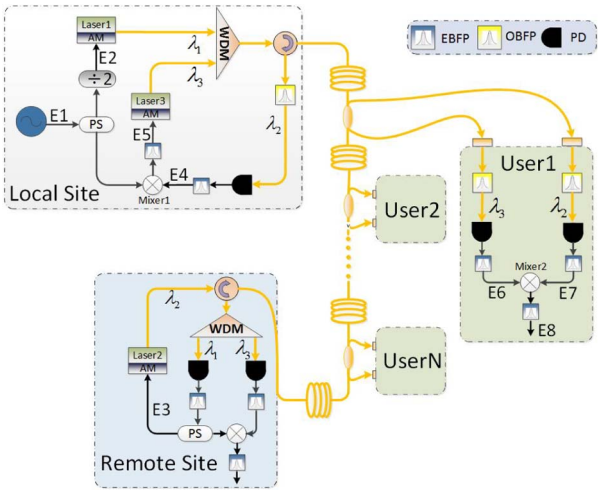

Fig. 1. Schematic of the proposed multi-access frequency transfer system with passive phase noise compensation. EBPF, electric bandpass filter; OBPF, optical bandpass filter; PD, photodetector; PS, power splitter; AM, amplitude modulator.

the same fiber link on another wavelength (λ_2) to efficiently suppress the impact of backscattering. It is worth noting that an optical reflector or circulator can also be used to return the signal directly on the same wavelength to obtain a better bidirectional symmetry at the cost of the impact of backscattering. The round-trip signal from the remote at the local site is detected by a photodetector (PD), and then mixed with the standard RF signal on the other branch to generate a phase-conjugated RF signal. The phase-conjugated RF signal is then modulated on the third wavelength (λ_3) and transmitted along the fiber link. At a user end, along the fiber link anywhere, parts of the forward signal of λ_3 and the backward signal of λ_2 are picked out through optical coupling and optical bandpass filtering. The two picked signals are photodetected and then mixed to get a stable frequency signal. A stable frequency signal can also be achieved at the remote site by photodetecting the signals carried on λ_1 and λ_3, and mixing them.

The standard frequency signal at the local site can be denoted as

$$E_1 \propto \cos(\omega_s t + \varphi_s), \tag{1}$$

where ω_s and φ_s represent the angular frequency and initial phase of the signal, respectively. After divided by two at one branch, we have

$$E_2 \propto \cos\left[\frac{1}{2}(\omega_s t + \varphi_s)\right]. \tag{2}$$

At the remote site, the received probe RF signal can be expressed as

$$E_3 \propto \cos\left[\frac{1}{2}\omega_s(t - \tau_{LR\lambda 1}) + \frac{1}{2}\varphi_s\right], \tag{3}$$

where $\tau_{LR\lambda 1}$ is the fiber link propagation delay in the λ_1 channel from the local site to the remote site.

At the local site, the round-trip probe signal (λ_2) is filtered out by an optical bandpass filter (OBPF). The photodetected RF signal can be expressed as

$$E_4 \propto \cos\left[\frac{1}{2}\omega_s(t - \tau_{LR\lambda 1} - \tau_{RL\lambda 2}) + \frac{1}{2}\varphi_s\right], \tag{4}$$

where $\tau_{RL\lambda 2}$ is the fiber link propagation delay in the λ_2 channel from the remote site to the local site. After mixing with the standard signal at another branch and filtering out the down-converted RF signal, we have

$$E_5 \propto \cos\left[\frac{1}{2}\omega_s(t + \tau_{LR\lambda 1} + \tau_{RL\lambda 2}) + \frac{1}{2}\varphi_s\right]. \tag{5}$$

At each user end, the two photodetected RF signals can be expressed as

$$E_6 \propto \cos\left[\frac{1}{2}\omega_s(t + \tau_{LR\lambda 1} + \tau_{RL\lambda 2} - \tau_{LU\lambda 3}) + \frac{1}{2}\varphi_s\right], \tag{6}$$

$$E_7 \propto \cos\left[\frac{1}{2}\omega_s(t - \tau_{LR\lambda 1} - \tau_{RU\lambda 2}) + \frac{1}{2}\varphi_s\right], \tag{7}$$

where $\tau_{LU\lambda 3}$ is the fiber link propagation delay in the λ_3 channel from the local site to the user end. $\tau_{RU\lambda 2}$ is the fiber link propagation delay in the λ_2 channel from the remote site to the user end. By mixing E_6 with E_7, and filtering out the upper converted RF signal, we get

$$E_8 \propto \cos\left[\omega_s t - \frac{1}{2}\omega_s(\tau_{LU\lambda 3} - \tau_{UL\lambda 2}) + \varphi_s\right]. \tag{8}$$

In Eq. (8), we see that the fiber link propagation delay in the λ_1 channel, $\tau_{LR\lambda 1}$, has been cancelled. There is only residual phase noise, the second term in the bracket, caused by the asymmetry propagation delay of λ_2 and λ_3 along the fiber link from the local site to the user end. The influence of the residual phase noise for the bidirectional asymmetry can be neglected when the wavelength gap is small enough [15]; then we can reproduce the standard frequency signal at the user end. Similarly, the standard frequency signal can also be reproduced at the remote site.

The experimental setup is shown in Fig. 2. A 1 GHz RF signal from a microwave generator locked to a 10 MHz reference (Oscilloquartz SA OCXO 8607) is used as the standard frequency signal at the local site. The local remote sites are

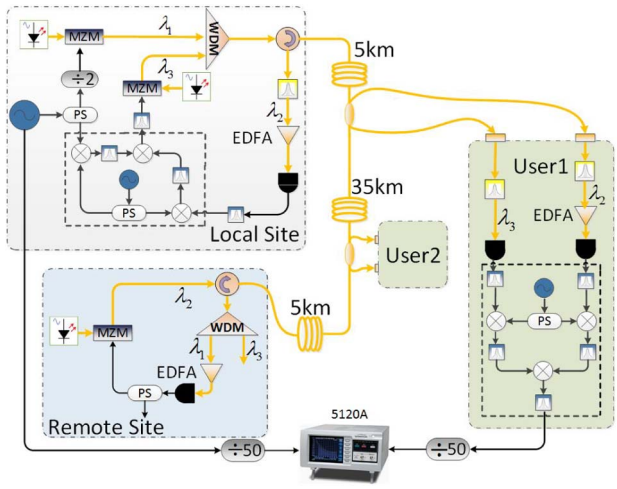

Fig. 2. Experiment setup of the proposed multi-access frequency transfer.

connected by a 45 km fiber link (consisting of 5, 35, and 5 km single mode fiber spools jointed by two 2 × 2 optical couplers). Two user ends are located at 5 and 40 km far from the local site along the fiber link, respectively. The wavelengths of λ_1, λ_2, and λ_3 launched from three CW lasers are 1549.32, 1550.98, and 1550.12 nm, respectively. Each RF signal to be transmitted along a fiber is modulated on the corresponding optical carrier by a Mach–Zehnder modulator. The bandwidth of PDs employed at each site is 1.2 GHz. The standard frequency signal and the reproduced signal at each user end are divided to 20 MHz, and then input to a phase noise test set (Symmetricom Inc., TSC5120A) for the performance evaluation of frequency transfer. The experimental system is in an ordinary air-conditioning room with an hourly temperature fluctuation of more than 3°C.

Consider the limited isolation and the nonlinearity of RF mixers, in practice, leaked input signals and their harmonics exist at the output ports of mixers. In our experiment, in order to suppress the effect of the leaked signals or their harmonics, the dual frequency mixer (DFM) scheme [6,8], shown by a dotted line in Fig. 2, is adopted at the local site and the user ends. In the DFM, the two input signals are first mixed with a local signal. The two outputs from the two mixers are filtered and mixed to get the wanted signal. The frequency of the output wanted signals from each mixer can be shifted to be different from those of the input signals and their harmonics by selecting the frequency of the local signal. Therefore, the impact of the leaked signals or their harmonics on the wanted output signal can be suppressed efficiently. At the local site, the frequency of the local signal for the DFM is set to 300 MHz. The two input signals of the DFM (the standard signal and the round-trip signal) are 1 GHz and 500 MHz, respectively. One can find that the wanted output signal from each mixer in the DFM has an enough frequency difference relative to the corresponding input signals and their harmonics in this case. Therefore, we can get a clear wanted output signal from each mixer by suitable filtering and, finally, obtain a clear phase-conjugated 500 MHz signal after the DFM. At the user ends, a 200 MHz signal is used as the local signal of the DFM to suppress the influence of the second harmonic of the two input 500 MHz signals on the wanted 1 GHz output signal.

Figure 3 shows the phase noise spectra of fiber-optic frequency transfer measured at the two user ends of 40 (a) and 5 km (b) far from the local site under different configurations. The results over a back-to-back link with a 1 m fiber is also presented, which is the phase noise floor of our experimental system and mainly determined by RF signal processes, optical modulation, and detection at each site. In the free running, the 1 GHz standard frequency signal at the local site is directly transferred to each user end over the fiber link. From Fig. 3(a), one sees that phase noise of the 40 km free-running link is significantly higher than the noise floor within 1 Hz offset frequency due to the fiber delay fluctuation, mainly induced by ambient variations. After about 4 k Hz, the higher phase noise of a 40 km link than that of the 1 m fiber is mainly due to the higher correlated phase noise between the standard frequency signal and its delayed signal for longer fiber distance. There are spurs at the offset frequency between 10 and 2 kHz under each configuration, which may mainly come from the microwave synthesizer and circuits in our system. Compared to the free running, we see that the phase noises caused by fiber delay

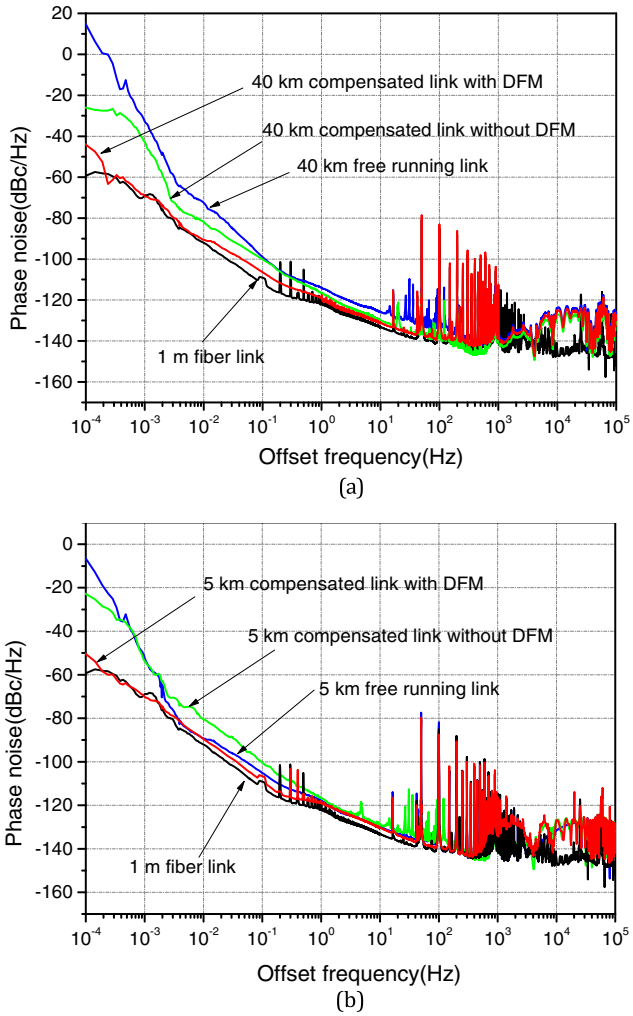

Fig. 3. Measured phase noise spectra of fiber-optic frequency transfer at the user ends of (a) 40 and (b) 5 km far from the local site with phase noise compensation with/without the DFM; free running.

fluctuation (mainly within 1 Hz) is significantly suppressed by using the phase compensation with the DFM (about 55 dBc/Hz at 0.0001 Hz, 40 dBc/Hz at 0.00 1 Hz, and 20 dBc/Hz at 0.01 Hz). The phase noise under compensation with the DFM has been almost equal to that of a 1 m fiber link, and mainly restricted by the noise floor. Moreover, we see that the scheme with the DFM obviously outperforms the scheme without the DFM in terms of the phase noise compensation (about −45 dBc/Hz versus −25 dBc/Hz at 0.0001 Hz, and −90 dBc/Hz versus −80 dBc/Hz at 0.01 Hz). The main reason is the influence of the leak signals and/or harmonics is efficiently suppressed by the DFM. In Fig. 3(b), similar results can be observed. A signal with relative phase noise close to the noise floor is also achieved at the 5 km user end by phase noise compensation with the DFM. A main difference is that the compensated 5 km link without the DFM has worse phase noises than that of the corresponding free-running link when the offset frequency is within about 0.002–1 Hz. It is mainly because the impact of the leaked signals and/or harmonics has exceeded that of ambient variation on the propagation delay of the free-running link, which is decreased with the decrease of

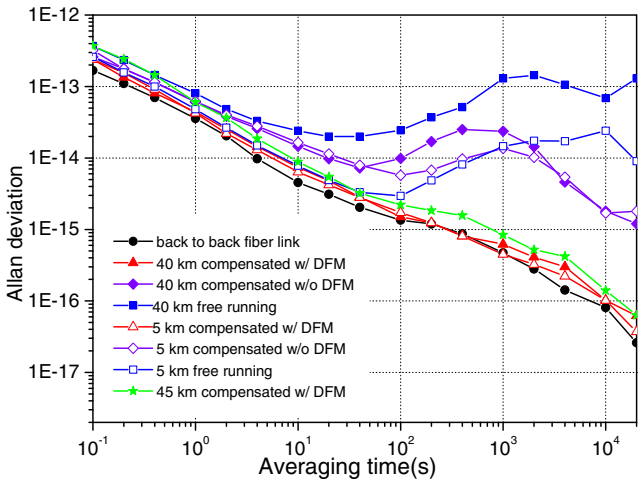

Fig. 4. Measured Allan deviation of fiber-optic frequency transfer in different system configurations.

the fiber link length. As the increase of ambient variation amplitude with the increase of time, the phase noise of a 5 km free link will increase with the decrease of offset frequency and, finally, may exceed that of the compensated link without the DFM after a certain offset frequency (about 0.0005 Hz in the figure).

The relative stability (Allan deviation) of each frequency transfer link in Fig. 3 with a 5 Hz measurement bandwidth is shown in Fig. 4. The Allan deviation of the 45 km link at the remote site is also shown in the figure. One sees that the signals with relative stabilities close to the floor of our system connected by a 1 m fiber (black line with solid dot) are achieved at the 5 km user end (4.2 e-14/1 s; 3.7 e-17/20,000 s), 40 km user end (4.4 e-14/1 s; 6.2 e-17/20,000 s) and the remote site (6.1 e-14/s; 6.3 e-17/20,000 s) when passive phase noise compensation with the DFM is adopted. Compared to the corresponding free-running link, the long-term stability of the 40 and 5 km compensated link with the DFM is improved significantly (about three orders and two orders for the 40 and 5 km compensated link with the DFM, respectively, at the average time of 20,000 s). The results indicate that the fiber delay fluctuation for the ambient variations has been compensated efficiently since the ambient variations are slow and, hence, mainly affect the long-term stabilities of fiber link. The bump on the Allan deviation curve of each compensated link with the DFM at the average time between 100 and 10,000 s is mainly attributed to the residual phase noise introduced by the delay fluctuation of components out of the compensation loop. High-performance devices and the temperature control of each site can be used to suppress the effect of components out of the compensation loop. For the compensated links without the DFM, the leaked signals and their harmonics seriously deteriorate the relative stabilities of fiber-optic frequency transfer (especially in long-term, more than one order at 20,000 s in our experiment), which even become worse than that of the free-running link at a 5 km user end at the average time within 1000 s.

In summary, we have proposed a multi-access fiber-optic RF dissemination with passive phase noise cancelation. Both the forward phase-conjugated signal at the local site and the stable frequency signal at arbitrary point are achieved by simple frequency mixing. The effect of backscattering is efficiently suppressed, and the bidirectional symmetry can also be guaranteed for a link with multiple user ends by using two different wavelengths for forward and backward directions and one common wavelength for all users. A multi-access frequency transfer with two user ends based on the proposed scheme is demonstrated over a 45 km fiber link. In the experiment, a DFM scheme is adopted to eliminate the impact of the leaked signals and their harmonics during frequency mixing. The radio frequency signals reproduced at the two user ends both have relative frequency stabilities at $10^{-17}/20,000$ s level.

Funding. National Natural Science Foundation of China (NSFC) (61627817, 61535006); Natural Science Foundation of Zhejiang Province (LY17F050003).

REFERENCES

1. S. M. Foreman, K. W. Holman, D. D. Hudson, D. J. Jones, and J. Ye, Rev. Sci. Instrum. **78**, 021101 (2007).
2. L. Sliwczynski, P. Krehlik, and M. Lipinski, Meas. Sci. Technol. **21**, 075302 (2010).
3. O. Lopez, A. Amy-Klein, C. Daussy, C. Chardonnet, F. Narbonneau, M. Lours, and G. Santarelli, Eur. Phys. J. D **48**, 35 (2008).
4. L. Sliwczynski, P. Krehlik, L. Buczek, and M. Lipinski, IEEE Trans. Instrum. Meas. **60**, 1480 (2011).
5. B. Wang, C. Gao, W. Chen, J. Miao, X. Zhu, Y. Bai, J. Zhang, Y. Feng, T. Li, and L. Wang, Sci. Rep. **2**, 556 (2012).
6. Y. He, B. J. Orr, K. G. Baldwin, M. J. Wouters, A. N. Luiten, G. Aben, and R. B. Warrington, Opt. Express **21**, 18754 (2013).
7. J. Wei, F. Zhang, Y. Zhou, D. Ben, and S. Pan, Opt. Lett. **39**, 3360 (2014).
8. F. Yin, A. Zhang, Y. Dai, T. Ren, K. Xu, J. Li, J. Lin, and G. Tang, Opt. Express **22**, 878 (2014).
9. Z. Wu, Y. Dai, F. Yin, K. Xu, J. Li, and J. Lin, Opt. Lett. **38**, 1098 (2013).
10. W. Li, W. T. Wang, W. H. Sun, W. Y. Wang, and N. H. Zhu, Opt. Lett. **39**, 4294 (2014).
11. G. Grosche, Opt. Lett. **39**, 2545 (2014).
12. C. Gao, B. Wang, W. Chen, Y. Bai, J. Miao, X. Zhu, T. Li, and L. Wang, Opt. Lett. **37**, 4690 (2012).
13. S. W. Schediwy, D. Gozzard, K. G. Baldwin, B. J. Orr, R. B. Warrington, G. Aben, and A. N. Luiten, Opt. Lett. **38**, 2893 (2013).
14. Y. Bai, B. Wang, C. Gao, J. Miao, X. Zhu, and L. Wang, Chin. Opt. Lett. **13**, 061201 (2015).
15. L. Yu, R. Wang, L. Lu, Y. Zhu, J. Zheng, C. Wu, B. Zhang, and P. Wang, Opt. Express **23**, 19783 (2015).
16. B. Wang, X. Zhu, C. Gao, Y. Bai, J. Dong, and L. Wang, Sci. Rep. **5**, 13851 (2015).

202.120.39.147 {ts '2018-05-19 22:41:47'}